DTIC COPY

REPORT DOCUMENTATION PAGE

Form Approved
OMB No. 0704-0188

1. REPORT DATE (DD-MM-YYYY)	2. REPORT TYPE	3. DATES COVERED (From - To)
31-Oct-2007	REPRINT	20-Oct-06-20-Oct-07

4. TITLE AND SUBTITLE
Modeling the Effects of Atmospheric Propagation for Spectral Libraries of Natural Backgrounds

5a. CONTRACT NUMBER
FA8718-05-C-0084

5b. GRANT NUMBER

5c. PROGRAM ELEMENT NUMBER
62601F

6. AUTHOR(S)
Mary Ann Glennon, Gail Anderson, Dimitris Manolakis, Ronald Lockwood, Peggy Grigsby, John Jacobson, John Cipar, Thomas Cooley

5d. PROJECT NUMBER
1010

5e. TASK NUMBER
BS

5f. WORK UNIT NUMBER
A1

7. PERFORMING ORGANIZATION NAME(S) AND ADDRESS(ES)
Boston College
Institute for Scientific Research
St. Clement's Hall
140 Commonwealth Ave.
Chestnut Hill, MA 02467-3862

8. PERFORMING ORGANIZATION REPORT NUMBER

9. SPONSORING / MONITORING AGENCY NAME(S) AND ADDRESS(ES)
Air Force Research Laboratory
29 Randolph Road
Hanscom AFB, MA 01731-3010

10. SPONSOR/MONITOR'S ACRONYM(S)
AFRL/RVBYM

11. SPONSOR/MONITOR'S REPORT NUMBER(S)
AFRL-RV-HA-TR-2007-1194

12. DISTRIBUTION / AVAILABILITY STATEMENT
Approved for Public Release; distribution unlimited

13. SUPPLEMENTARY NOTES
Reprint from the SPIE Defense and Security Symposium. Proc. of SPIE Vol. 6565 656521, (2007). The paper was cleared by AFRL (VS07.004-932 - ESC 07-0332) prior to submission.

14. ABSTRACT :
The statistics of natural backgrounds extracted from an Airborne Visible and Infrared Imaging Spectrometer (AVIRIS) hyperspectral datacube collected over Fort AP Hill, VA, were used to demonstrate the effects of the two atmospheric components of a statistical end-to-end performance prediction model. New capabilities in MODTRAN™5 were used to generate coefficients for linear transformations used in the atmospheric transmission and compensation components of a typical end-to-end model. Model radiance statistics, calculated using reflectance data, is found to be similar to the original AVIRIS radiance data. Moreover, if identical atmospheric conditions are applied in the atmospheric transmission and in the atmospheric compensation model components and the effects of sensor noise are disregarded, the resulting reflectance statistics are identical to the original reflectance statistics.

15. SUBJECT TERMS
Hyperspectral, AVIRIS, Atmospheric Compensation, MODTRAN, spectral variability

16. SECURITY CLASSIFICATION OF:			17. LIMITATION OF ABSTRACT	18. NUMBER OF PAGES	19a. NAME OF RESPONSIBLE PERSON
a. REPORT	b. ABSTRACT	c. THIS PAGE			Brian Lemay, 1Lt, USAF
U	U	U	SAR	9	19b. TELEPHONE NUMBER (include area code) 781-377-0303

Modeling the Effects of Atmospheric Propagation for Spectral Libraries of Natural Backgrounds

Mary Ann Glennon*[a], Gail Anderson[b], Dimitris Manolakis[c], Ronald Lockwood[b], Peggy Grigsby[d], John Jacobson[d], John Cipar[b], Thomas Cooley[e]
[a]Boston College, Institute for Scientific Research, Chestnut Hill, MA 02467
[b]Air Force Research Laboratory, 29 Randolph Road, Hanscom AFB, MA 01731-3010
[c]MIT Lincoln Laboratory, 244 Wood Street, Lexington, MA 02420
[d]National Air and Space Intelligence Center, 4180 Watson Way, Wright Patterson AFB, OH 45433
[e]Air Force Research Laboratory, 3500 Aberdeen Ave SE, Kirtland AFB, NM 87117-5776

Abstract

The statistics of natural backgrounds extracted from an Airborne Visible and Infrared Imaging Spectrometer (AVIRIS) hyperspectral datacube collected over Fort AP Hill, VA, were used to demonstrate the effects of the two atmospheric components of a statistical end-to-end performance prediction model. New capabilities in MODTRAN™5 were used to generate coefficients for linear transformations used in the atmospheric transmission and compensation components of a typical end-to-end model. Model radiance statistics, calculated using reflectance data, is found to be similar to the original AVIRIS radiance data. Moreover, if identical atmospheric conditions are applied in the atmospheric transmission and in the atmospheric compensation model components and the effects of sensor noise are disregarded, the resulting reflectance statistics are identical to the original reflectance statistics.

Keywords: Hyperspectral, AVIRIS, Atmospheric Compensation, MODTRAN, spectral variability

1. Introduction

The reflectance spectra of natural backgrounds are often assumed to be drawn from a multivariate normal population. However, recent work has shown that even for background populations carefully screened using clustering algorithms, statistical descriptions of hyperspectral data exhibit long-tail behavior that cannot be accounted for by normal distribution models[1]. Instead, statistical properties of natural hyperspectral backgrounds have been effectively modeled with distinct combinations of Gaussian body and *t*-elliptically contoured distributions, representing the heaviness of the tails[1].

Realistic probability density functions are essential for accurate target detection prediction capabilities and image classification algorithms[1,2,3]. The design and performance evaluation of target detection algorithms for hyperspectral imaging sensors depend on the characteristics of target and background distributions. In general, the target spectral signatures are obtained from spectral libraries and the background statistics are estimated from the available hyperspectral data. For performance prediction, statistical models for both the spectral variability of the involved targets and backgrounds are needed.

Performance prediction algorithms that rely on statistics derived from hyperspectral scenes[4,5], rather than physics-based algorithms[6], apply linear transformations to model sensor noise[4,5] and atmospheric conditions[5] prior to performance prediction algorithms. Input first and second order statistics, the mean and covariance matrix, can be extracted from hyperspectral imagery to describe the material variability. Figure 1 illustrates the processing flow for an end-to-end model. In this model, input reflectance statistics are converted to at-sensor radiance using a radiative transport model, such as MODTRAN™ [7,8]. Sensor noise can be added to the resulting radiance statistics, followed by removal of the atmospheric contaminants to simulate a real world processing sequence. The goal of this paper is to examine the effects of the atmospheric transmission/compensation doublet on the spectral variability of natural backgrounds. Specifically, statistics derived from Airborne Visible and Infrared Imaging Spectrometer (AVIRIS) imagery will be used to illustrate the effects of atmospheric transmission and compensation.

*mary.glennon.ctr@hanscom.af.mil; phone 781-377-7868

2. Methodology

Following the approach used by the FLAASH algorithm[9], the relationship between model at-sensor radiance, $L(\lambda)$, and pixel surface reflectance, $\rho(\lambda)$, is given by:

$$L(\lambda) = \frac{A(\lambda)\rho(\lambda)}{(1-\rho_a(\lambda)S(\lambda))} + \frac{B(\lambda)\rho_a(\lambda)}{(1-\rho_a(\lambda)S(\lambda))} + L_p(\lambda) \qquad (1)$$

where λ represents the central wavelengths of the discrete spectral channels as measured by the hyperspectral sensor, $\rho(\lambda)$ is the pixel reflectance, $\rho_a(\lambda)$ is a spatially averaged reflectance of an area surrounding the pixel of interest (used to correct for effects of light scattered from the scene into the field of view of the senor, e.g., the adjacency effect), $S(\lambda)$ is the spherical albedo, and $L_p(\lambda)$ is the backscattered radiance. The pixel reflectance is assumed to be Lambertian.

Atmospheric quantities, $A(\lambda)$ and $B(\lambda)$, are the product of the top-of-atmosphere solar downward horizontal flux, total sun-to-ground transmittance, and cosine of the solar zenith angle. Furthermore, $A(\lambda)$ also includes the direct transmission from observer to sun while $B(\lambda)$, includes the medium embedded diffuse transmittance. Thus, the $A(\lambda)$ and $B(\lambda)$ terms are surface independent coefficients that vary only with atmospheric and geometric conditions. The first term in equation (1) corresponds to the radiance reaching the surface (from both sky-shine and direct solar illumination) that is backscattered directly into the sensor, while the second term corresponds to the radiance from the surface that is re-scattered by the atmosphere into the sensor (Figure 2).

With the release of MODTRAN™5[7, 8], the atmospheric contributions to at-sensor radiance (A, B, L_p and S) in equation (1) can be calculated with a single MODTRAN run using the new DISORT option for atmospheric correction. This option exploits the reciprocity principle of radiation transport theory[7, 8]. Equation 1 shows that the conversion from pixel reflectance to at-sensor radiance is a linear function, dependant upon the spectrum of the pixel of interest, the spatially averaged background spectrum to account for the adjacency effect and the atmospheric conditions, defined by the visibility (or aerosol content), water column density, scene and sensor geometry. Thus the transformation from pixel reflectance to at-sensor-radiance can be expressed using a simple linear equation given by:

$$L(\lambda) = c(\lambda)\rho(\lambda) + d(\lambda) \qquad (2)$$

where vectors $c(\lambda)$ and $d(\lambda)$ depend only on atmospheric vectors, $A(\lambda)$, $B(\lambda)$, and $S(\lambda)$ calculated using MODTRAN™, and the spatially averaged reflectance, $\rho_a(\lambda)$:

$$c(\lambda) = \frac{A(\lambda)}{(1-\rho_a(\lambda)S(\lambda))} \qquad (3)$$

and

$$d(\lambda) = \frac{B(\lambda)}{(1-\rho_a(\lambda)S(\lambda)} + L_p(\lambda) \qquad (4)$$

Spectral library statistics, include the material mean and covariance matrix, are estimated from the datacube. The mean reflectance, $\hat{\rho}(\lambda)$, is given by:

$$\hat{\rho}(\lambda) = \frac{1}{N}\sum_{i=1}^{N}\rho_i(\lambda) \qquad (5)$$

and, the covariance, Γ, is given by:

$$\Gamma = \frac{1}{N}\sum_{i=1}^{N}(\rho_i(\lambda) - \hat{\rho}(\lambda))(\rho_i(\lambda) - \hat{\rho}(\lambda)) \quad (6)$$

The Mahanalobis distance, Δ^2, given by:

$$\Delta^2 = (\rho(\lambda) - \hat{\rho}(\lambda))\Gamma^{-1}(\rho(\lambda) - \hat{\rho}(\lambda)) \quad (7)$$

was also estimated from the data. The probability of exceeding the Mahanalobis distance was then determined empirically and used as a means to compare statistical distributions.

Of more practical importance to statistical performance prediction models, the reflectance covariance matrix, can be transformed to radiance statistics using the relationship:

$$\Gamma_{radiance} = \mathbf{C}\Gamma_{\mathrm{Re}\,flectance}\mathbf{C}^T \quad (8)$$

where

$$\mathbf{C} = diag\{c(\lambda_1),\ldots,c(\lambda_n)\} \quad (9)$$

The correlation coefficient matrix (R) is given by:

$$R = \frac{\Gamma_{ij}}{\sqrt{\Gamma_{ii}\Gamma_{jj}}} \quad (10)$$

Note that R is independent of atmospheric state. R is of importance because the probability density function for a multivariate t-ECD, used to model the statistical variability of hyperspectral data, is a function of the material reflectance, the correlation coefficient matrix and the number of degrees of freedom[2]. For the case where $\Gamma_B \neq \Gamma_T$, the target can be modeled with a Gaussian model because the probability of detection depends upon the body of the target distribution and not the tails[2,3].

3. Data Description

We use hyperspectral data collected with the AVIRIS sensor over Fort AP Hill in September, 2001 (Figure 3). Fort AP Hill is typical of a fairly rural northeast forest with both deciduous and coniferous tree stands. The AVIRIS instrument is sensitive from 375 to 2500 nm in 224 spectral channels with a nominal bandwidth of about 10nm. Data were calibrated to at-sensor radiance and distortions due to aircraft motion were removed by JPL. The sensor was flown on the Twin Otter aircraft in low-altitude nadir-looking configuration, providing a GSD of approximately 3.5m.

Calibrated radiance was atmospherically corrected to reflectance using the MODTRAN-based Fast Line of Sight Analysis of Atmospheric Spectral Hypercubes (FLAASH)[9]. Water vapor was retrieved from the radiance cube using the 940 nm water vapor absorption region separately for each pixel in the scene. FLAASH calculated the average water vapor at 1400 atm-cm. The scene-averaged visibility or aerosol overburden is calculated using a reflectance ratio-based algorithm based upon an empirical model by Kaufman[10]. For the Fort AP Hill scene, the average visibility was calculated at 122 km.

The spectral library data used for this study was extracted from the FLAASH reflectance cube using spectrally distinct classes reported by Cipar and others[11]. The unsupervised classification algorithm[11] determines cluster centers with a modified migrating means technique to separate the dense parts of the hyperspectral data cloud. A total of 19 classes were reported by Cipar and others[11]. Two distinct classes were chosen for this experiment with sufficient pixels to provide a good estimate of the mean and covariance matrix. A total of 13,808 pixels lie within class 6 and are highlighted in blue in Figure 3b. From visual inspection and personal site inspections, class 6 appears to consist mainly of grass and other low-lying vegetation. Class #2 (in red) was identified[11] as a deciduous class and consists of 32,593 pixels. Spectral channels with low signal to noise ratios and those near the strong water absorption features near 1350 and 1900 nm were removed from further calculations, leaving 155 "good" channels for analysis.

4. Results

Scene and atmospheric conditions used as input to MODTRAN to calculate the atmospheric constants in Equation 1 (A, B, S, and L_p) are listed in Table 1. The visibility and scene-averaged water column were retrieved by FLAASH during the original atmospheric compensation step. For all calculations, the spatially averaged reflectance, ρ_a , in equation (1), was defined as the reflectance mean of the entire scene. Note that FLAASH both retrieves the water column totals and calculates the spatially averaged reflectance, ρ_a, separately for each pixel in the scene. In contrast, the MODTRAN model parameters used in this study, including water content and ρ_a, are identical for each pixel.

We first apply equation (1) to each pixel in the atmospherically corrected reflectance datacube using the 155 'good' spectral channels and the model atmosphere (Table 1) to produce a model radiance datacube, $\hat{L}$. Pixel spectra were extracted from the model radiance cube, $\hat{L}$, and the original AVIRIS radiance cube, L, for each class and the mean and covariance estimated. Finally, the Mahanalobis distance is computed. The statistics extracted from the model radiance, $\hat{L}$, were compared to that of the original AVIRIS calibrated radiance, L.

The class means calculated using the original AVIRIS radiance dataset and the model radiance cube are very similar (Figure 4) for both classes. Differences between the two means for each class are generally less than 2% and are nearly identical. Larger differences are observed at discrete bands associated with atmospheric absorption regions at 940, 1130 nm and at the edges of the opaque atmospheric windows near 1460 and 1750 nm. Given that the FLAASH algorithm retrieved water vapor amounts at each pixel and that equation (1) uses a single water vapor, these variations are not surprising. Within each class, variations in water vapor are predicted by the FLAASH algorithm. For example, for the pixels within the grass class, the mean water vapor was estimated at 1448 atm-cm with a standard deviation of 48 atm-cm, slightly higher than the estimate for the whole cube. In addition, both methodologies assume a uniform visibility across the scene and a standard mid-latitude summer aerosol model. It is conceivable that aerosols may change across a scene. Furthermore, more sophisticated aerosol models, such as a power law distribution, may provide more accurate at-sensor radiance estimates[12].

Equation 10 predicts that if the atmospheric model was exactly correct for this scene, then the correlation matrix for the model radiance data and the original AVIRIS data cube should be nearly identical. In reality, the atmospheric model in (1) is a simplified description of the actual atmospheric parameters, such as effects of aerosol and water vapor. Nevertheless, differences between model and actual correlation coefficients are less than 5% for over 93% of the matrix. In all cases, the larger correlation coefficient differences are associated with spectral channels in the water vapor absorption regions.

The empirical exceedence distributions of Mahanalobis distance for each class are used as another tool to evaluate differences between the model radiance and the original AVIRIS radiance. This metric has been used to characterize the statistics of natural backgrounds imaged by hyperspectral sensors[1]. Similar to previous studies[1], the distributions of Mahanalobis distance for both classes do not follow the normal distribution (Figure 5). Instead, the heavy tails exhibited by the grass and deciduous classes are very similar to the original data. The original radiance data, plotted as dotted curves, exhibit higher Mahanalobis distances for lower probabilities of exceedence than does the model data, suggesting that the variability in the model data is slightly reduced relative to the original dataset. Although no effort was made to characterize the heavy tails for either distribution, the differences are predicted to be small.

In the above discussion, pixels within each class are used to calculate the means and the covariances for both the model and original radiances. For statistical models, however, the atmosphere is propagated directly onto material statistics (mean and covariance) extracted from a library. For each class, the difference between mean radiances and covariances calculated using the two sources are less than 0.1%

In the end-to-end performance tool depicted in Figure 1, the atmospheric compensation step removes the contamination of the atmosphere from model radiance statistics prior to performance statistics calculations. If identical atmospheric parameters are used to compensate the model radiance using the inverse of equation 3, then the resulting reflectance means and covariance statistics will be identical to the original input statistics, excluding the effects of sensor noise. If the errors associated with atmospheric compensation are to be modeled, then different atmospheric conditions must be used to calculate the constants in equation 1 for use in the atmospheric compensation step.

The differences between the AVIRIS radiance and model radiance class means (Figure 4) can be considered an upper bound to errors due to atmospheric compensation and are generally less than 5%. The AVIRIS data used in this study was collected under nearly ideal conditions for hyperspectral imagery; clear to moderate aerosol/haze, low to moderate water vapor and nadir viewing geometries. Surface reflectance produced with the FLAASH algorithm has been compared with high accuracy[13] to ground spectral measurements under similar conditions. More stressing scenarios, such as scenes collected with an off-nadir geometry, scenes with higher water content and/or lower visibilities (heavy aerosol conditions) may exhibit larger errors when the linear algorithms for atmospheric transmission and compensation are applied. Further analysis of hyperspectral datacubes collected with varying conditions is needed to understand the limitations of this formulation of the radiance equation.

Table 1

Scene Parameters	Original Scenario
Latitude, Longitude	38.125 N, 77.325 W
Atmospheric Model	Mid-Latitude Summer
Sensor Altitude	3.55 km
Time (UTC)	15.40
Visibility (km)	122
Water Column	1400 atm-cm

Summary

The statistics of natural backgrounds extracted from an AVIRIS hyperspectral datacube collected over Fort AP Hill, VA, were used to demonstrate the effects of the two atmospheric components (transmission and compensation) of a statistical end-to-end performance prediction model. First, new capabilities in MODTRAN™5 were used to generate coefficients for the linear transformation used in the atmospheric transmission component of a typical end-to-end performance prediction model. Statistics extracted from the model radiance cube were compared to that of the original AVIRIS radiance cube. Class means differed by less than 3-5% in regions outside of the atmospheric absorption bands. Distributions of Mahanalobis distance for both datasets are also very similar. Furthermore, for the scene used in this study, if identical atmospheric conditions are used in the linear transformation to reflectance, the resulting reflectance statistics are identical to the original reflectance statistics.

Acknowledgements

The authors would like to thank John Grossman and Alexander Berk for the discussions on the formulations for A and B in equation (1). The authors would like to thank Robert Green and Jessica Faust of NASA/JPL for providing the data and performing the aircraft and instrument calibrations. Gerald Felde and Tamilyn Becker did the FLAASH atmospheric compensation calculations.

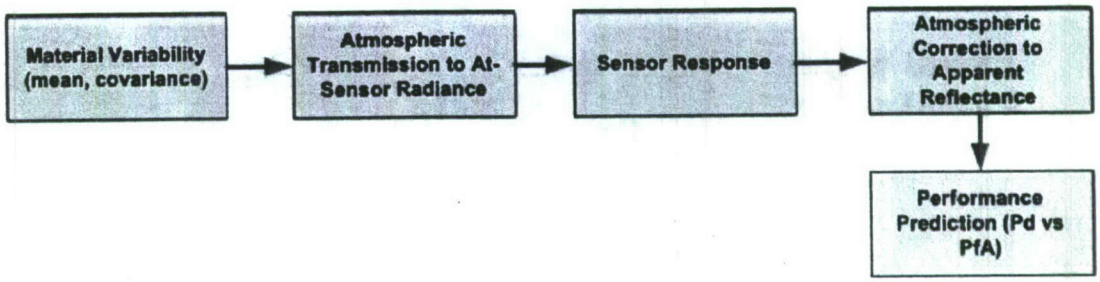

Figure 1. Procedures for end-to-end performance prediction models

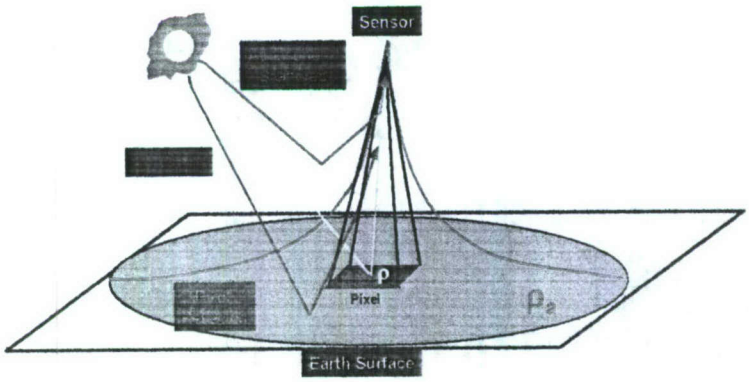

Figure 2. Illustration of contributions to the target pixel upwelling radiance. The yellow line segment corresponds to the radiance backscattered directly into the sensor from the pixel of interest, the blue arrow corresponds to radiance reflected by the earth's surface surrounding the pixel and backscattered into the sensor. The green arrow corresponds to radiance backscattered by the atmosphere without reaching the surface.

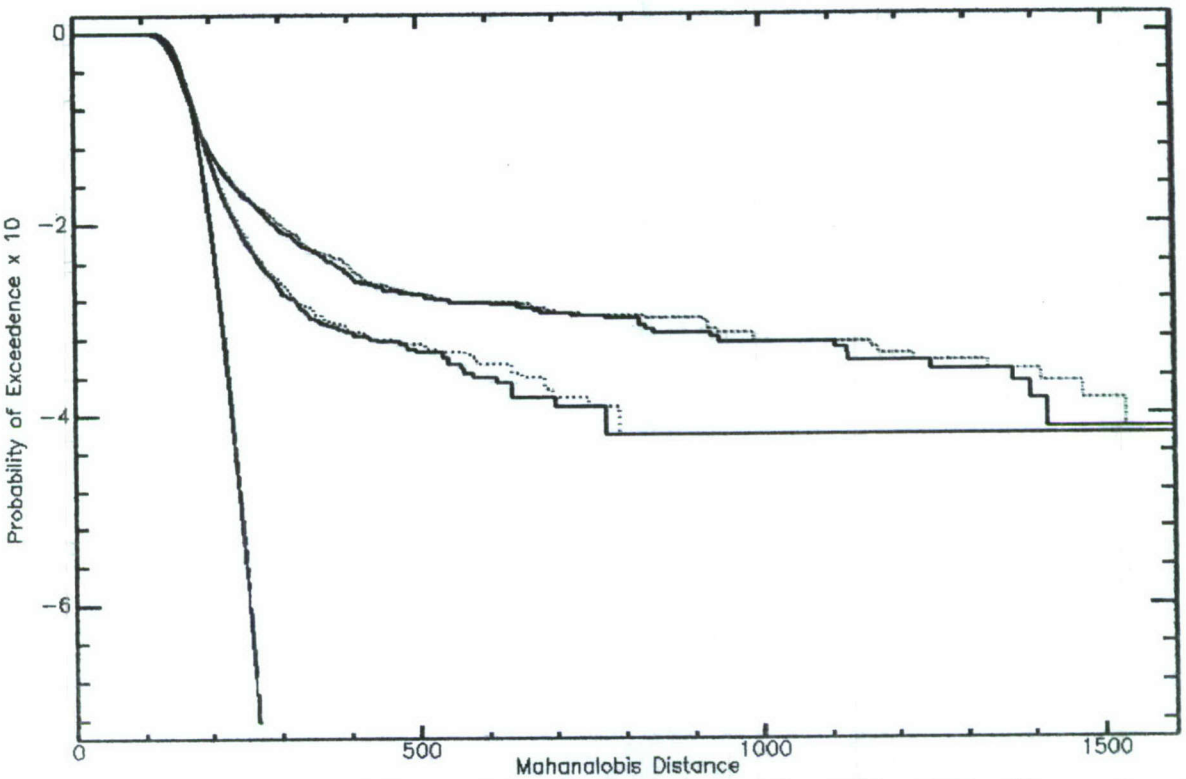

Figure 5. The distribution of Mahanalobis distance calculated for the spectral classes shown in Figure 3. The solid curves represent the distribution using the model radiance and the dotted curves use the original AVIRIS radiance cube. Red and blue curves are associated with class 2 (deciduous) and class 6 (grass), respectively. The abscissa was truncated at a Mahanalobis distance of 1600 for clarity. The black curve represents the normal distribution model.